NEW MECHANISMS OF CHARM PRODUCTION*

Antoni Szczurek

The Henryk Niewodniczański Institute of Nuclear Physics
Polish Academy of Sciences
Radzikowskiego 152, 31-342 Kraków, Poland
and
Rzeszów University, Rejtana 16A, 35-959 Rzeszów, Poland

(Received May 8, 2012)

We discuss production of charm quarks, mesons as well as nonphotonic electrons in pp scattering at RHIC. The distributions in rapidity and transverse momentum of charm and bottom quarks/antiquarks are calculated in the $k_{\rm t}$-factorization approach. The hadronization of heavy quarks is done by means of phenomenological fragmentation functions and semileptonic decay functions are found by fitting semileptonic decay data. Good description of the inclusive data at large transverse momenta of electrons is obtained and a missing strength at small transverse momenta of electrons is found. In addition, we discuss kinematical correlations between charged leptons from different mechanisms. Reactions initiated by purely QED $\gamma^*\gamma^*$-fusion in elastic and inelastic pp collisions as well as diffractive mechanism of exclusive $c\bar{c}$ production are included. A good description of the dilepton invariant mass spectrum of the PHENIX Collaboration is achieved. Distributions in the dilepton pair transverse momentum and in azimuthal angle between electron and positron are presented. A new mechanism of exclusive production of $c\bar{c}$ is discussed. Corresponding results are shown and the possibility of its identification is discussed. We discuss also production of two pairs of $c\bar{c}$ within a simple formalism of double-parton scattering (DPS). Very large cross sections, comparable to single-$c\bar{c}$ production, are predicted for LHC energies. Both total inclusive cross section as a function of energy and differential distributions are shown. We discuss a perspective how to identify the double scattering contribution.

DOI:10.5506/APhysPolB.43.1623
PACS numbers: 12.38.–t, 12.38.Cy, 14.65.Dw

* Presented at the Cracow Epiphany Conference on Present and Future of B Physics, Cracow, Poland, January 9–11, 2012.

1. Introduction

In recent years, the PHENIX and STAR collaborations have measured transverse momentum distribution of so-called nonphotonic electrons [1, 2]. The dominant contribution to the nonphotonic electrons/positrons comes from the semileptonic decays of charm and/or beauty mesons. Formally such processes can be divided into three subsequent stages. First $c\bar{c}$ or $b\bar{b}$ quarks are produced. The dominant mechanisms being gluon–gluon fusion at higher energies or quark–antiquark annihilation close to the threshold. Next, the heavy quarks/antiquarks fragment into heavy charmed mesons D, D^* or B, B^*. The vector D^* and B^* mesons decay strongly producing pseudoscalar D and B mesons. Finally, the heavy pseudoscalar mesons decay semileptonically producing electrons/positrons.

The hadronization of heavy quarks is usually done with the help of phenomenological fragmentation functions with parameters adjusted to the production of heavy mesons in e^+e^- or $p\bar{p}$ collisions.

The last ingredient are semileptonic decays of heavy mesons. Only recently the CLEO [3] and BaBar [4] collaborations have measured precise spectra of electrons/positrons coming from the decays of D and B mesons. This is done by producing specific resonances: $\Psi(3770)$ which decays into D and $\bar{D}$ mesons (CLEO) and $\Upsilon(4S)$ which decays into B and $\bar{B}$ mesons (BaBar). In both cases the heavy mesons are almost at rest, so in practice one measures the meson rest frame distributions of electrons/positrons.

In this presentation, the results for production of electrons have been obtained within the $k_{\rm t}$-factorization approach. At relatively low RHIC energies, intermediate x-values of gluon distributions become relevant. The Kwieciński unintegrated gluon (parton) distributions seem the best suited in this context [8]. We use both Peterson [9] and so-called perturbative [10] fragmentation functions. The electron/positron decay functions fitted recently [12] to the recent CLEO and BaBar data are used.

Recently, the PHENIX Collaboration has measured dilepton invariant mass spectrum from 0 to 8 GeV in pp collisions at $\sqrt{s} = 200$ GeV [7]. Up to now, production of open charm and bottom was studied only in inclusive measurements of charmed mesons [5] and electrons [6], and only inclusive observables were calculated in pQCD approach [11, 12].

Some time ago, we have studied kinematical correlations of $c\bar{c}$ quarks [14], which is, however, difficult to study experimentally. High luminosity and, in a consequence, better statistics at present colliders opens a new possibility to study not only inclusive distributions but also correlations between outgoing particles. Kinematical correlations constitute an alternative method to pin down the cross section for charm and bottom production.

In this presentation I shall show some selected results obtained in [12, 13].

Recently, we have studied a new mechanism of exclusive production of $c\bar{c}$ pairs [20]. In such a process, a single pair of $c\bar{c}$ is produced together with associated two protons. We shall comment on a possibility to identify the peculiar mechanism. The original presentation at the conference included also inclusive diffractive processes.

With growing energy the heavy quark–antiquark production becomes sensitive to lower-x gluon distributions. At high energies, a possibility of two pairs of $c\bar{c}$ production opens up [21]. We comment on which areas of the phase space are potentially interesting in order to pin down the double parton scattering contribution.

2. Inclusive production of $c\bar{c}$

2.1. Formalism

We consider the reaction $h_1 + h_2 \to Q + \bar{Q} + X$, where Q and $\bar{Q}$ are heavy quark and heavy antiquark, respectively.

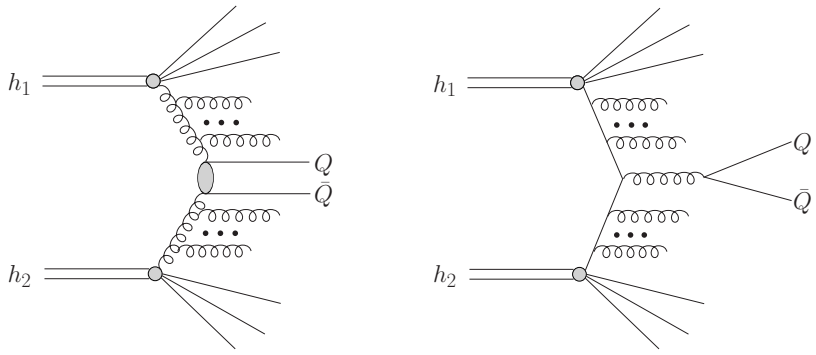

Fig. 1. Basic diagrams relevant for gluon–gluon fusion (left panel) and quark–antiquark annihilation (right panel) in the $k_{\rm t}$-factorization approach.

In the $k_{\rm t}$-factorization approach the differential cross section reads

$$\frac{d\sigma}{dy_1 dy_2 d^2p_{1,\rm t} d^2p_{2,\rm t}} = \sum_{i,j} \int \frac{d^2\kappa_{1,\rm t}}{\pi} \frac{d^2\kappa_{2,\rm t}}{\pi} \frac{1}{16\pi^2 (x_1 x_2 s)^2} \overline{|\mathcal{M}_{ij}|^2}$$
$$\delta^2\left(\vec{\kappa}_{1,\rm t} + \vec{\kappa}_{2,\rm t} - \vec{p}_{1,\rm t} - \vec{p}_{2,\rm t}\right) \mathcal{F}_i\left(x_1, \kappa^2_{1,\rm t}\right) \mathcal{F}_j\left(x_2, \kappa^2_{2,\rm t}\right) , \qquad (1)$$

where $\mathcal{F}_i(x_1, \kappa^2_{1,\rm t})$ and $\mathcal{F}_j(x_2, \kappa^2_{2,\rm t})$ are the so-called unintegrated gluon (parton) distributions. Leading-order matrix elements for off-shell gluons [15] were used. The two-dimensional Dirac delta function assures momentum conservation. The unintegrated parton distributions are evaluated at

$$x_1 = \frac{m_{1,\mathrm{t}}}{\sqrt{s}} \exp(y_1) + \frac{m_{2,\mathrm{t}}}{\sqrt{s}} \exp(y_2) ,$$
$$x_2 = \frac{m_{1,\mathrm{t}}}{\sqrt{s}} \exp(-y_1) + \frac{m_{2,\mathrm{t}}}{\sqrt{s}} \exp(-y_2) ,$$

where $m_{i,\mathrm{t}} = \sqrt{p_{i,\mathrm{t}}^2 + m_Q^2}$.

Introducing new variables $\vec{Q}_\mathrm{t} = \vec{\kappa}_{1,\mathrm{t}} + \vec{\kappa}_{2,\mathrm{t}}$, $\vec{q}_\mathrm{t} = \vec{\kappa}_{1,\mathrm{t}} - \vec{\kappa}_{2,\mathrm{t}}$ one can write

$$\frac{d\sigma_{ij}}{dy_1 dy_2 d^2p_{1,\mathrm{t}} d^2p_{2,\mathrm{t}}} = \int d^2q_\mathrm{t} \, \frac{1}{4\pi^2} \frac{1}{16\pi^2 (x_1 x_2 s)^2} \, \overline{|\mathcal{M}_{ij}|^2} \, \mathcal{F}_i\left(x_1, \kappa_{1,\mathrm{t}}^2\right) \, \mathcal{F}_j\left(x_2, \kappa_{2,\mathrm{t}}^2\right) . \tag{2}$$

This formula is very useful to study correlations between the produced heavy quark Q and heavy antiquark $\bar{Q}$ [14].

At the Tevatron and LHC energies the contribution of the $gg \to Q\bar{Q}$ subprocess is more than one order of magnitude larger than its counterpart for the $q\bar{q} \to Q\bar{Q}$ subprocess. At RHIC energy the relative contribution of the $q\bar{q}$ annihilation is somewhat bigger. Therefore in the following, we shall take into account not only gluon–gluon fusion process but also the quark–antiquark annihilation mechanism.

The production of electrons/positrons is a multi-step process. The whole procedure of electron/positron production can be written in the following schematic way

$$\frac{d\sigma^e}{dy d^2p} = \frac{d\sigma^Q}{dy d^2p} \otimes D_{Q\to D} \otimes f_{D\to e} , \tag{3}$$

where the symbol $\otimes$ denotes a convolution of the different distributions. The first term is responsible for production of heavy quarks/antiquarks. Next step is the process of formation of heavy mesons. We follow a phenomenological approach and take *e.g.* Peterson [9], and Braaten *et al.* [10] fragmentation functions with parameters from the literature [16]. The electron decay function accounts for the proper branching fractions.

The inclusive distributions of hadrons can be calculated as a convolution of inclusive distributions of heavy quarks/antiquarks and $Q \to h$ fragmentation functions

$$\frac{d\sigma\left(y_1, p_{1\mathrm{t}}^H, y_2, p_{2\mathrm{t}}^H, \phi\right)}{dy_1 dp_{1\mathrm{t}}^H dy_2 dp_{2\mathrm{t}}^H d\phi} \approx \int \frac{D_{Q\to H}(z_1)}{z_1} \, \frac{D_{\bar{Q}\to \bar{H}}(z_2)}{z_2} \times \frac{d\sigma\left(y_1, p_{1\mathrm{t}}^Q, y_2, p_{2\mathrm{t}}^Q, \phi\right)}{dy_1 dp_{1\mathrm{t}}^Q dy_2 dp_{2\mathrm{t}}^Q d\phi} dz_1 dz_2 , \tag{4}$$

where $p_{1\mathrm{t}}^Q = \frac{p_{1\mathrm{t}}^H}{z_1}$, $p_{2\mathrm{t}}^Q = \frac{p_{2\mathrm{t}}^H}{z_2}$, with meson longitudinal fractions $z_1, z_2 \in (0, 1)$.

We use decay functions fitted recently [12] to the CLEO and BaBar data. In our approach, the electrons (positrons) are generated isotropically in the heavy meson rest frame.

2.2. Results

2.2.1. Single electron spectra

Before we start presenting our single particle distributions, let us focus on the decay functions discussed shortly above. In Fig. 2, we show our fit [12] to the CLEO and BaBar data. The good quality fit of the data allows to obtain reliable predictions for electron/positron single particle spectra.

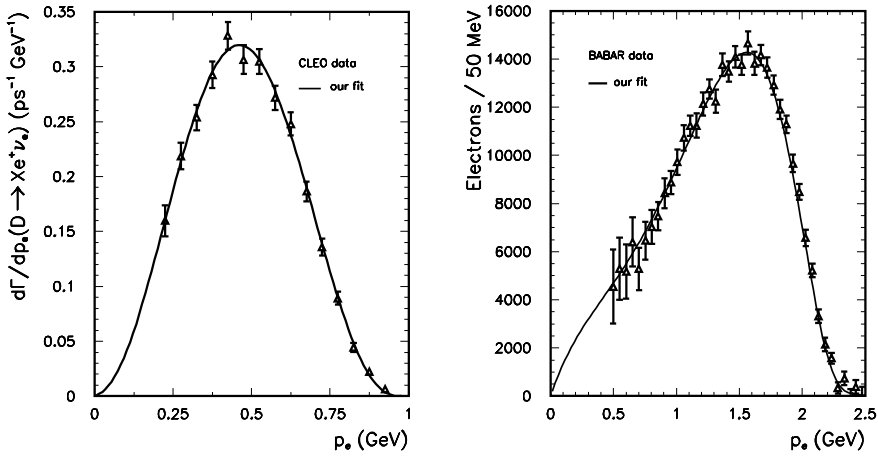

Fig. 2. Our fit to the CLEO [3] and BaBar [4] data.

Now we shall focus on transverse momentum distribution of electrons/positrons measured recently by the STAR and PHENIX collaborations at RHIC [1, 2]. In Fig. 3, as an example, we show results obtained with the Kwieciński UPDFs [8]. In Ref. [12], we have discussed in addition other UGDFs. Uncertainties due to different combinations of factorization and renormalization scales as well as due to different choices fragmentation functions are shown in Fig. 4. In these calculations, we have included both gluon–gluon fusion as well as quark–antiquark annihilation. In the last case, we use matrix elements with on-shell formula but for off-shell kinematics (the discussion of this point can be found in our earlier paper [14]). In Ref. [12], we have discussed also uncertainties due to the choice of quark masses.

Study of nonphotonic $e^{\pm}$ and hadron correlations allows to "extract" a fractional contribution of the bottom mesons $B/(D+B)$ as a function of electron/positron transverse momentum [17]. Recently, the STAR Collaboration has extended the measurement of the relative B contribution to

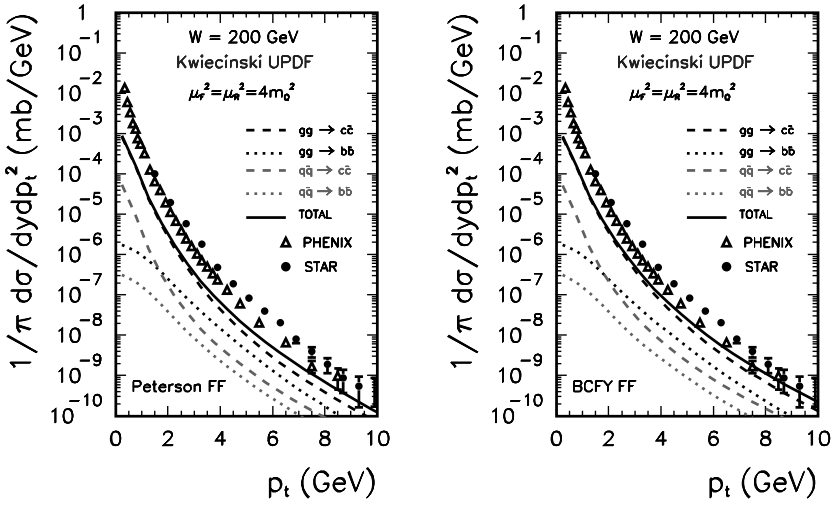

Fig. 3. Transverse momentum distribution of electrons/positrons obtained with the Kwieciński UPDFs. We show separately contributions of the gluon–gluon fusion (black) and quark–antiquark annihilation (grey). On the left side, results with the Peterson fragmentation functions and on the right side, with BCFY fragmentation functions.

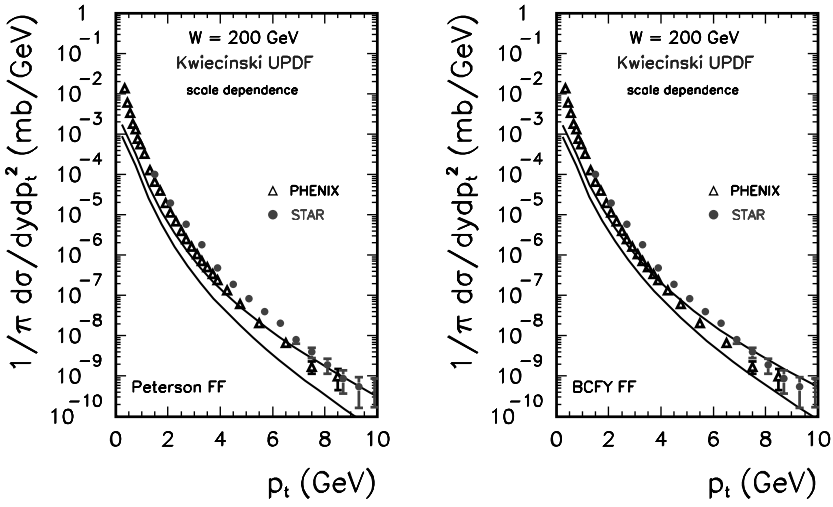

Fig. 4. Factorization and renormalization uncertainty band of our k_t-factorization calculation with unintegrated Kwieciński gluon, quark and antiquark distributions for the Peterson fragmentation function (left panel) and BCFY fragmentation function (right panel). The open triangles represent the PHENIX Collaboration data and the solid circles the STAR Collaboration data.

electron/positron transverse momenta ~ 10 GeV [18]. In Fig. 5 (Kwieciński UPDFs) shown are results for different scales and different fragmentation functions. There is a strong dependence on the factorization and renormalization scale. A slightly better agreement is obtained with the Peterson fragmentation functions.

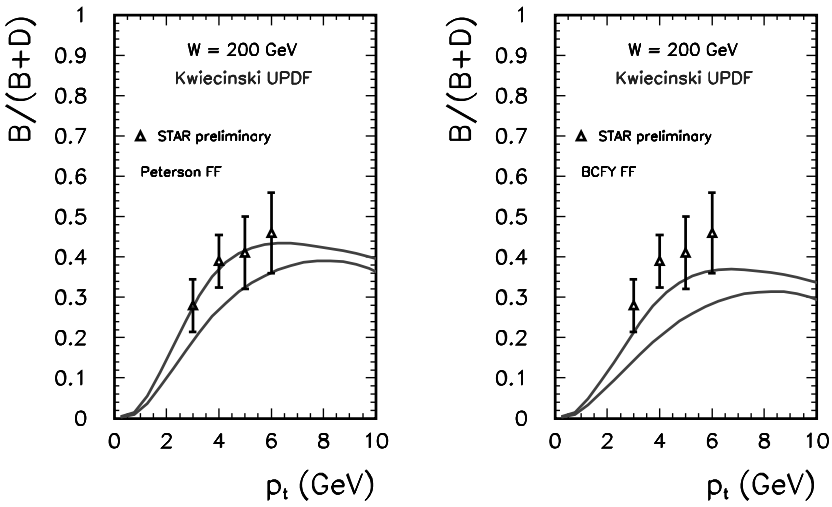

Fig. 5. The fraction of the B decays for the Kwieciński UPDFs. The uncertainty band due to the choice of the scales is shown for the Peterson (left) and Braaten *et al.* (right) fragmentation functions. Both gluon–gluon fusion as well as quark–antiquark annihilation are included in this calculation.

2.2.2. Electron–positron correlations

When calculating correlation observables, we have included also processes shown in Fig. 6 and Fig. 7. The photon–photon induced processes were first included in Ref. [13]. The central exclusive diffractive process shown in Fig. 7 was proposed in Ref. [20].

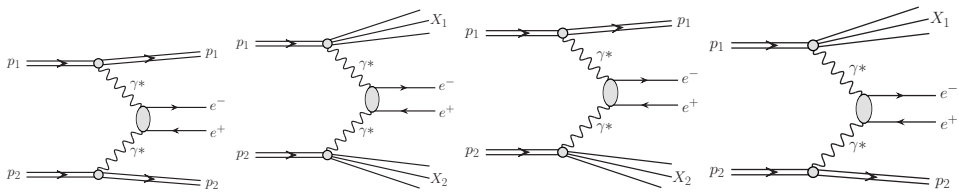

Fig. 6. Diagrammatic representation of processes initiated by photon–photon subprocesses: double-elastic, double-inelastic, inelastic–elastic and elastic–inelastic.

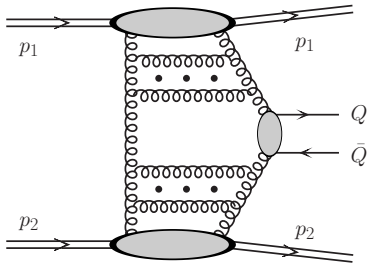

Fig. 7. The mechanism of exclusive double-diffractive production of open charm.

In Fig. 8, we show e^+e^- invariant mass distributions calculated with the Kwieciński (left) and KMR (right) UGDFs. One can clearly see that both the Kwieciński and KMR [22] UGDFs give fairly good description of the data for $M_{e^+e^-} > 3$ GeV. At small invariant masses the Kwieciński UGDF underestimates the PHENIX data and the KMR UGDF starts to overestimate the data points below $M_{e^+e^-} = 2$ GeV.

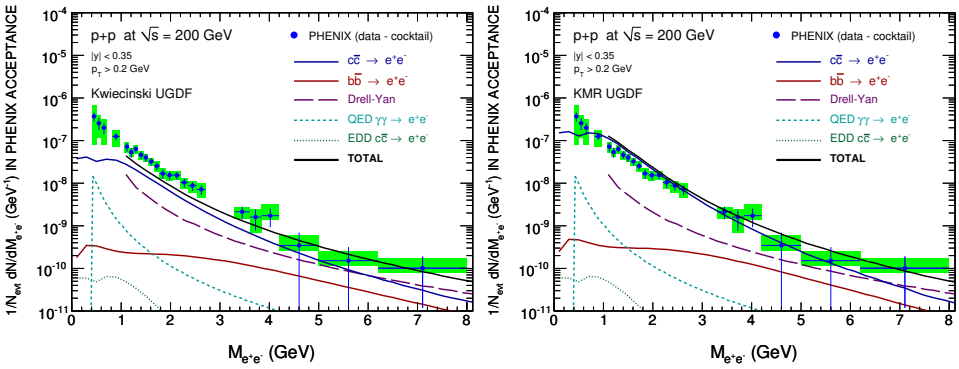

Fig. 8. Dielectron invariant mass distribution for pp collisions at $\sqrt{s} = 200$ GeV for the Kwieciński (left) and KMR (right) UGDFs. Different contributions are shown separately: semileptonic decay of charm by the middle (blue) solid line, semileptonic decay of bottom by the lowest (red) solid line, Drell–Yan mechanism by the long-dashed (purple) line, gamma–gamma processes by the dashed (blue) line and the central diffractive contribution by the dotted (green) line at the bottom. In this calculation, we have included azimuthal angle acceptance of the PHENIX detector [7].

In Fig. 9, we show uncertainties related to the contribution of semileptonic decays. The left panel presents uncertainties due to the factorization scale variation as described in the figure caption. The right panel shows uncertainties due to the modification of the heavy quark masses.

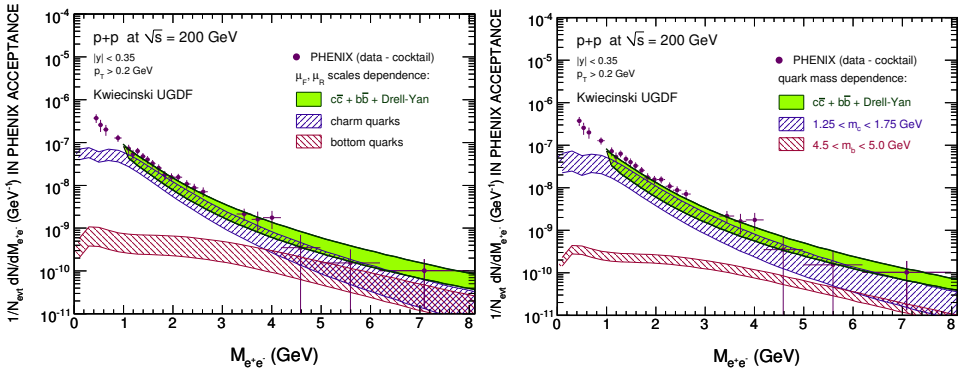

Fig. 9. The uncertainties of theoretical calculations. The left panel shows the factorization scale uncertainties, the lower curve corresponds to $\mu_{\rm F}^2, \mu_{\rm R}^2 = m_{1,\rm t}^2 + m_{2,\rm t}^2$ and the upper curve to $\mu_{\rm R}^2 = k_{\rm t}^2$, $\mu_{\rm F}^2 = 4m_Q^2$, where $k_{\rm t}$ is gluon transverse momentum. The right panel shows the quark mass uncertainties as indicated in the figure.

If the detector can measure both transverse momenta of electron/positron and their directions, one can construct a distribution in transverse momentum of the dielectron pair: $\vec{p}_{\rm t,sum} = \vec{p}_{1\rm t} + \vec{p}_{2\rm t}$. Our predictions, including the semileptonic decays and Drell–Yan processes, are shown in the left panel of Fig. 10. Both processes give rather similar distributions. The distributions of this type were not measured so far experimentally. The distribution in $p_{\rm t,sum}$ is not only a consequence of gluon transverse momenta but involves also fragmentation process and semileptonic decays. With good azimuthal

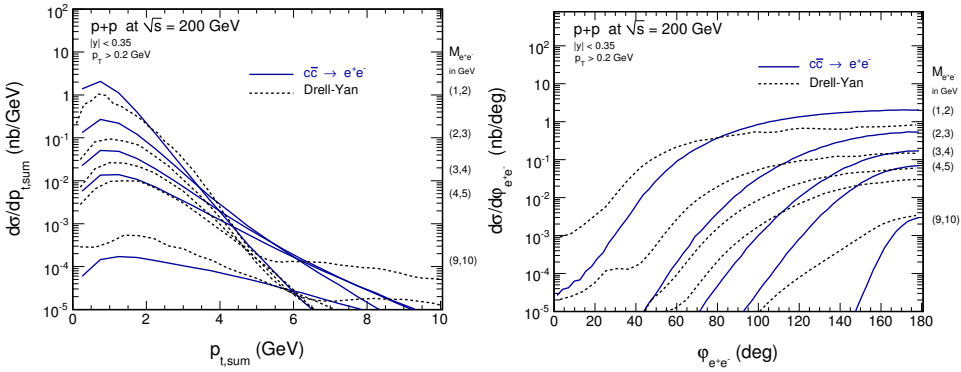

Fig. 10. Distribution in transverse momentum of the dielectron pair (left) and in azimuthal angle between electron and positron (right) for semileptonic decays (solid line) and Drell–Yan processes (dashed line). Here Kwieciński UGDF and Peterson fragmentation function were used.

resolution of detectors one could also construct distribution in azimuthal angle between electron and positron. Corresponding predictions are shown in the right panel of Fig. 10. One can see an interesting dependence on the invariant mass of the dielectron pair — the smaller the invariant mass the larger the decorrelation in azimuthal angle.

3. Exclusive diffractive production of $c\bar{c}$

Central exclusive mechanisms of $c\bar{c}$ production at high energies shown in Fig. 7 constitutes a special category of diffractive processes. In this case, the central system X is produced in the color singlet state. This leads to rapidity gaps between forward/backward produced protons and the central system. The QCD mechanism of central exclusive heavy quark–antiquark dijets (in particularly $b\bar{b}$) is a source of the irreducible background to the exclusive Higgs boson production [23, 24]. Central exclusive production of $c\bar{c}$ and $b\bar{b}$ pairs was studied in detail in our previous papers [20, 23, 24]. In these calculations, the $pp \to p(q\bar{q})p$ reaction was considered as a 4-body process with exact kinematics. The applied perturbative model of theoretical predictions is based on the Khoze–Martin–Ryskin (KMR) approach used previously for the exclusive Higgs boson production [25]. Total cross sections and differential distributions for heavy quarks are calculated by using $k_{\rm t}$-factorization approach with the help of off-diagonal unintegrated gluon distribution functions.

This QCD model works very well in the case of exclusive dijets and charmonia production [26, 27, 28, 29]. Here, we discuss the production of $c\bar{c}$ pairs. In practice, however, one measures rather charmed mesons. The measurement and its interpretation is, therefore, more complicated and will be not discussed here. Such experimental analyses are being performed now at the Tevatron and could be also available in Run II at RHIC. In this context, it is very interesting to compare the mechanism of central exclusive production of charm quarks with standard inclusive single and central diffractive processes.

As in the KMR approach [25, 30] the amplitude of the exclusive central diffractive $q\bar{q}$ pair production $pp \to p(q\bar{q})p$ can be written as

$$\mathcal{M}_{\lambda_q\lambda_{\bar{q}}} = \frac{s}{2}\,\frac{\pi^2\delta_{c_1c_2}}{N_c^2-1}\,{\rm Im}\int d^2q_{0,\rm t}\; V^{c_1c_2}_{\lambda_q\lambda_{\bar{q}}}(q_1,q_2,k_1,k_2) \times \frac{f^{\rm off}_{g,1}\left(x_1,x_1',q^2_{0,\rm t},q^2_{1,\rm t},t_1\right) f^{\rm off}_{g,2}\left(x_2,x_2',q^2_{0,\rm t},q^2_{2,\rm t},t_2\right)}{q^2_{0,\rm t}\,q^2_{1,\rm t}\,q^2_{2,\rm t}}\,, \tag{5}$$

where λ_q, $\lambda_{\bar{q}}$ are helicities of heavy q and $\bar{q}$, respectively, $t_{1,2}$ are the momentum transfers along each proton line, $q_{1,\rm t}, q_{2,\rm t}, x_{1,2}$ and $q_{0,\rm t}$, $x_1' \sim x_2' \ll x_{1,2}$ are the transverse momenta and the longitudinal momentum fractions for

active and screening gluons, respectively. Above $f^{\rm off}_{g,1/2}$, there are the off-diagonal UGDFs related to both nucleons. The vertex factor $V^{c_1c_2}_{\lambda_q\lambda_{\bar q}}(q_1, q_2, k_1, k_2)$ is the production amplitude of a pair of massive quark q and antiquark $\bar q$ with helicities λ_q, $\lambda_{\bar q}$ and momenta k_1, k_2, respectively. The longitudinal momentum fractions of active gluons are calculated based on kinematical variables of outgoing quark and antiquark: $x_1 = \frac{m_{q,\rm t}}{\sqrt{s}} \exp(+y_q) + \frac{m_{\bar q,\rm t}}{\sqrt{s}} \exp(+y_{\bar q})$ and $x_2 = \frac{m_{q,\rm t}}{\sqrt{s}} \exp(-y_q) + \frac{m_{\bar q,\rm t}}{\sqrt{s}} \exp(-y_{\bar q})$, where $m_{q,\rm t}$ and $m_{\bar q,\rm t}$ are transverse masses of the quark and antiquark, respectively, and y_q and $y_{\bar q}$ are corresponding rapidities.

The off-diagonal UGDFs can be approximated as [31]

$$f^{\rm off}_g\left(x', x_{1,2}, q^2_{1,2\rm t}, q^2_{0,\rm t}, \mu^2_{\rm F}\right) \simeq R_g\, f_g\left(x_{1,2}, q^2_{1,2\rm t}, \mu^2_{\rm F}\right) . \tag{6}$$

The factor R_g here cannot be calculated from first principles in the most general case of off-diagonal UGDFs. It can be estimated only in the case of off-diagonal collinear PDFs when $x' \ll x$ and $xg = x^{-\lambda}(1-x)^n$, and then $R_g = \frac{2^{2\lambda+3}}{\sqrt{\pi}} \frac{\Gamma(\lambda+5/2)}{\Gamma(\lambda+4)}$. In the considered kinematics, the diagonal unintegrated densities can be written in terms of the conventional (integrated) densities $xg(x, q^2_{\rm t})$ as [31]

$$f_g\left(x, q^2_{\rm t}, \mu^2\right) = \frac{\partial}{\partial \ln q^2_{\rm t}} \left[xg\left(x, q^2_{\rm t}\right) \sqrt{T_g\left(q^2_{\rm t}, \mu^2\right)} \right] , \tag{7}$$

where T_g is the conventional Sudakov survival factor which suppresses real emissions from the active gluon during the evolution.

The hard subprocess $g^*g^* \to q\bar q$ amplitude $V^{c_1c_2}_{\lambda_q\lambda_{\bar q}}(q_1, q_2, k_1, k_2)$ reads

$$V^{c_1c_2,\,\mu\nu}_{\lambda_q\lambda_{\bar q}}(q_1, q_2, k_1, k_2) = -\frac{g_s^2}{2}\, \delta^{c_1c_2}\, \bar u_{\lambda_q}(k_1)$$
$$\left(\gamma^\nu \frac{\hat q_1 - \hat k_1 - m}{(q_1-k_1)^2 - m^2} \gamma^\mu - \gamma^\mu \frac{\hat q_1 - \hat k_2 + m}{(q_1-k_2)^2 - m^2} \gamma^\nu \right) v_{\lambda_{\bar q}}(k_2) . \tag{8}$$

In the present calculations, we use the GJR08 set of collinear gluon distributions [33]. In the analogy to the CEP of Higgs boson, where renormalization and factorization scales $\mu^2 = \mu^2_{\rm R} = \mu^2_{\rm F} = M^2_H$ are preferred, we take $\mu^2 = M^2_{c\bar c}$. Absorption corrections to the bare $pp \to p(q\bar q)p$ amplitude, which are necessary to be taken into account (to ensure exclusivity of the process), are included approximately by multiplying the cross section by the gap survival factors $S_{\rm G} = 0.1$ for RHIC and $S_{\rm G} = 0.03$ for the LHC energy. More details about exclusive production of heavy quarks can be found in our original paper [20]. Let us come now to presentation of our results.

In Fig. 11, we show rapidity distribution of c quarks from the exclusive mechanism (solid lines) shown already in Fig. 7. We show the results for LO (upper curves) and NLO (lower curves) collinear gluon distributions [33]. We observe large difference of results for LO and NLO gluon distributions especially at LHC. For comparison, we show the contribution of inclusive central diffractive component discussed in detail in [19]. In this calculation, we have included gap survival factors $S_{\rm G} = 0.1$ for $\sqrt{s} = 500$ GeV and $S_{\rm G} = 0.03$ for $\sqrt{s} = 14$ TeV. The cross section for the exclusive mechanism is similar to that for the inclusive central diffractive mechanism. The exclusive production starts to dominate only at large c quark rapidities. Therefore, a measurement of the cross section with double (both side) rapidity gaps may be not sufficient to single out the exclusive mechanism. Clearly other cuts would be necessary.

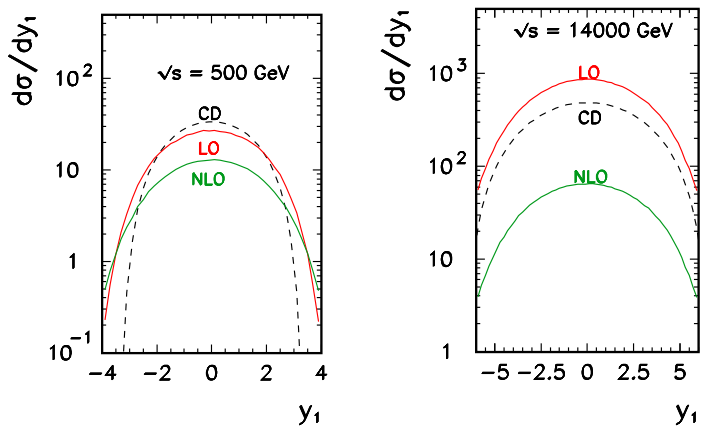

Fig. 11. Distributions in rapidity of c quark/antiquark for the exclusive component at $\sqrt{s} = 500$ GeV (left panel) and $\sqrt{s} = 14$ TeV (right panel). GJR08 collinear gluon distributions were used to obtain the unintegrated gluon distribution according to the KMR prescription. For comparison, we show the inclusive central diffractive contribution (dashed line).

Distributions in the c quark ($\bar{c}$ antiquark) transverse momentum are shown in Fig. 12. At RHIC energy distributions for both mechanisms have very similar shape. However, at LHC nominal energy we observe that inclusive central diffractive component extends to higher transverse momentum than that for the exclusive central diffractive one. In order to identify the exclusive component, a much more precise analysis of kinematical correlations between quark and antiquark is needed. A detailed Monte Carlo studies of final states of both mechanisms could help to find a criterion to separate experimentally the two dynamically different components.

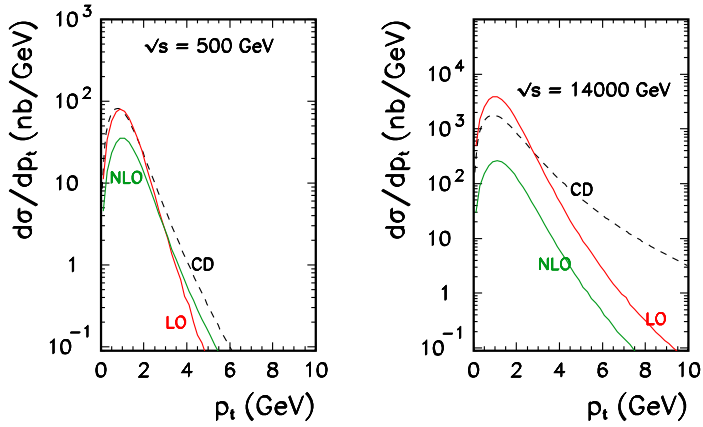

Fig. 12. Distributions in transverse momentum of c quark/antiquark for the exclusive component at $\sqrt{s} = 500$ GeV (left panel) and $\sqrt{s} = 14$ TeV (right panel). GJR08 collinear gluon distributions were used to obtain the unintegrated gluon distribution. For comparison, we show the inclusive central diffractive contribution (dashed line).

4. Double parton scattering production of $c\bar{c}c\bar{c}$

4.1. Framework

The double-parton scattering has been recognized long ago. Several estimates of the cross section for different processes have been presented in recent years. In the present analysis, we discuss production of $(c\bar{c})(c\bar{c})$ four-parton final state which has not been discussed so far but is particularly interesting especially in the context of experiments being carried out at LHC. A sketch of the mechanism is shown in Fig. 13.

The double-parton scattering formalism proposed so far assumes two single-parton scatterings. In a simple probabilistic picture, the cross section for double-parton scattering can be written as

$$\sigma^{\rm DPS}(pp \to c\bar{c}c\bar{c}X) = \frac{1}{2\sigma_{\rm eff}}\, \sigma^{\rm SPS}(pp \to c\bar{c}X_1)\, \sigma^{\rm SPS}(pp \to c\bar{c}X_2)\,. \quad (9)$$

This formula assumes that the two subprocesses are not correlated and do not interfere. At low energies, one has to include parton momentum conservation *i.e.* extra limitations: $x_1 + x_3 < 1$ and $x_2 + x_4 < 1$, where x_1 and x_3 are longitudinal momentum fractions of gluons emitted from one proton and x_2 and x_4 their counterpairs for gluons emitted from the second proton. Experimental data provide an estimate of $\sigma_{\rm eff}$ in the denominator of formula (9). In our analysis we take $\sigma_{\rm eff} = 15$ mb.

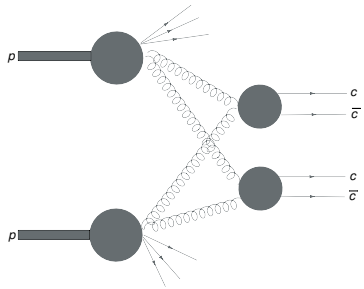

Fig. 13. Mechanism of $(c\bar{c})(c\bar{c})$ production via double-parton scattering.

The simple formula (9) can be generalized to include differential distributions. In the same approximation differential distribution can be written as

$$\frac{d\sigma}{dy_1 dy_2 d^2p_{1\mathrm{t}} dy_3 dy_4 d^2p_{2\mathrm{t}}} = \frac{1}{2\sigma_{\mathrm{eff}}} \frac{d\sigma}{dy_1 dy_2 d^2p_{1\mathrm{t}}} \frac{d\sigma}{dy_3 dy_4 d^2p_{2\mathrm{t}}} \tag{10}$$

which reproduces formula (9). This cross section is formally differential in 8 dimensions but can be easily reduced to 7 dimensions noting that physics of unpolarized scattering cannot depend on azimuthal angle of the pair or on azimuthal angle of one of the produced c ($\bar{c}$) quark (antiquark). The differential distributions for each single scattering step can be written in terms of collinear gluon distributions with longitudinal momentum fractions x_1, x_2, x_3 and x_4 expressed in terms of rapidities y_1, y_2, y_3, y_4 and transverse momenta of quark (or antiquark) for each step.

A slightly more general formula for the cross section can be written formally in terms of double-parton distributions (dPDF), *e.g.* F_{gg}, F_{qq}, *etc.* In the case of heavy quark (antiquark) production at high energies

$$d\sigma^{\mathrm{DPS}} = \frac{1}{2\sigma_{\mathrm{eff}}} F_{gg}\left(x_1, x_3, \mu_1^2, \mu_2^2\right) F_{gg}\left(x_2, x_4, \mu_1^2, \mu_2^2\right) d\sigma_{gg\to c\bar{c}}\left(x_1, x_2, \mu_1^2\right) d\sigma_{gg\to c\bar{c}}\left(x_3, x_4, \mu_2^2\right) dx_1 dx_2 dx_3 dx_4 \,. \tag{11}$$

The double-parton distributions in Eq. (11) are not well known. Usually, one assumes the factorized form and expresses them via standard distributions for SPS. Even if factorization is valid at some scale, QCD evolution leads to a factorization breaking [21].

In this presentation, we shall apply the commonly used factorized model. Some refinements are presented in [21].

4.2. Results

In Fig. 14 we compare cross sections for single $c\bar{c}$ and DPS $c\bar{c}c\bar{c}$ production as a function of pp center-of-mass energy. At low energies the cross section for $c\bar{c}$ is much larger. For reference, we show the proton–proton

total cross section as a function of energy. At low energy, the $c\bar{c}$ or $c\bar{c}c\bar{c}$ cross sections are much smaller than the total cross section. At higher energies the contributions approach the parametrized total cross section. This shows that inclusion of unitarity effect and/or saturation of parton distributions may be necessary. At LHC energies the cross section for both terms becomes comparable. This is a new situation when the double-parton scattering gives a large contribution to inclusive charm production. This issue was not discussed so far in the literature.

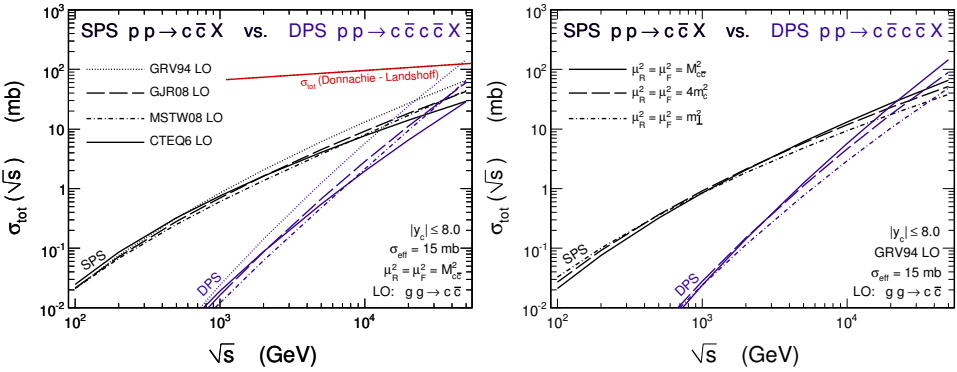

Fig. 14. Total LO cross section for single-parton and double-parton scattering as a function of center-of-mass energy (left panel) and uncertainties due to the choice of (factorization, renormalization) scales (right panel). We show, in addition, a parametrization of the total cross section in the left panel.

As an example, in Fig. 15, we present single c ($\bar{c}$) distributions. Within approximations discussed here the single-parton distributions are identical in shape for $c\bar{c}$ and $c\bar{c}c\bar{c}$. This means that double-scattering contribution produces naturally an extra energy-dependent K-factor to be contrasted with approximately energy-independent K-factor due to higher-order corrections. A strong dependence on the factorization and renormalization scales can be observed.

So far, we have discussed only single particle spectra of c or $\bar{c}$. A better test of DPS could be done by studying correlation observables. The correlations between c and $\bar{c}$ have been studied *e.g.* in [14]. In Fig. 16, we show distribution in the difference of c and $\bar{c}$ rapidities (left panel) as well as in the $c\bar{c}$ invariant mass $M_{c\bar{c}}$ (right panel). We show both cases: when $c\bar{c}$ are emitted in the same parton scattering ($c_1\bar{c}_2$ or $c_3\bar{c}_4$) and when they are emitted from different parton scatterings ($c_1\bar{c}_4$ or $c_2\bar{c}_3$). We observe a long tail for large rapidity difference as well as at large invariant masses of $c\bar{c}$. Such distributions for quarks and antiquarks cannot be directly measured. Instead their counterparts for mesons can be studied. This was discussed in more detail in our recent original paper [21].

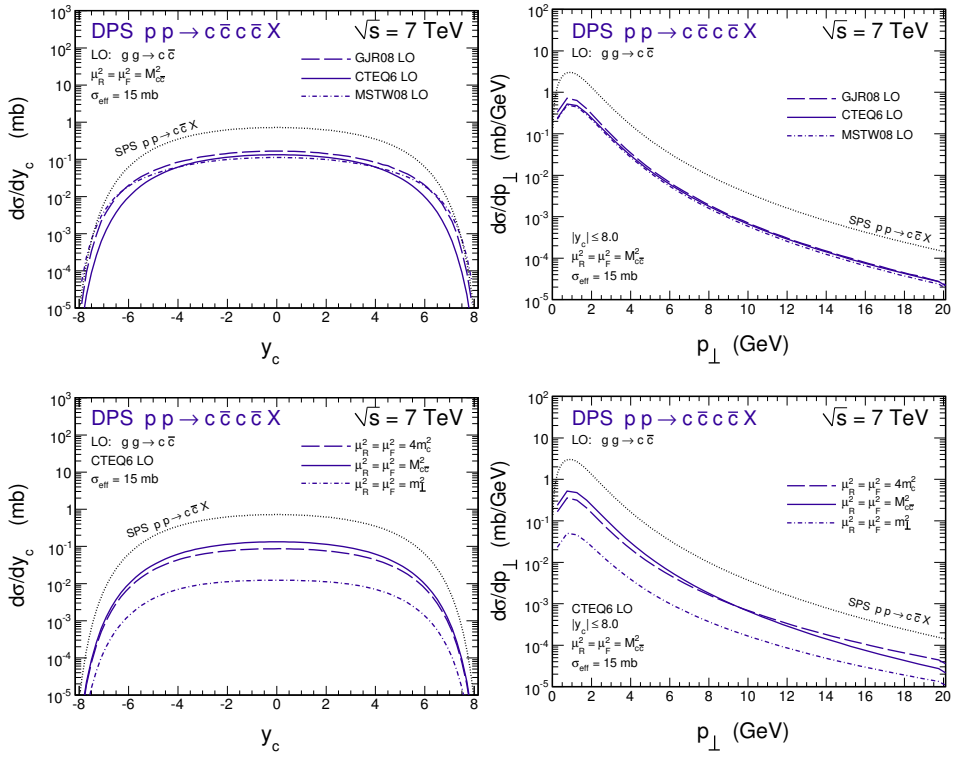

Fig. 15. Distribution in rapidity (left upper panel) and transverse momentum (right upper panel) for different UGDFs and associated uncertainties related to the choice of renormalization and factorization scales (lower panels) for c or $\bar{c}$ quarks at $\sqrt{s} =$ 7 TeV.

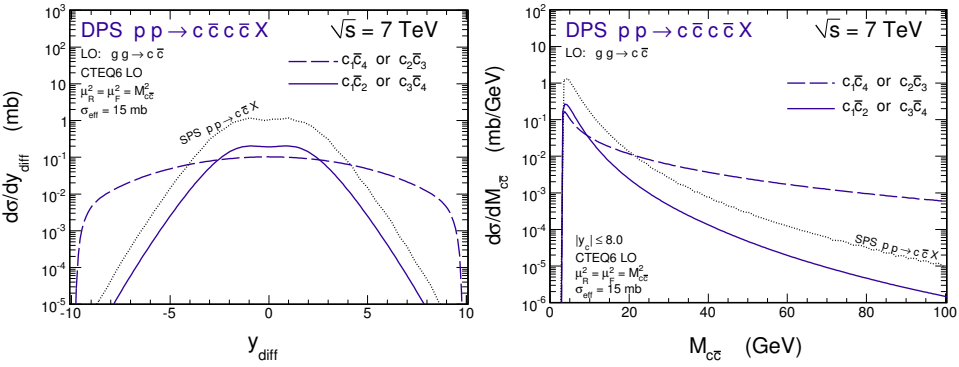

Fig. 16. Distribution in rapidity difference (left panel) and in invariant mass of the $c\bar{c}$ pair (right panel) at $\sqrt{s} = 7$ TeV.

As the last example, in Fig. 17, we present distribution in the transverse momentum of the $c\bar{c}$ pair $|\overrightarrow{p_{\perp c\bar{c}}}|$, where $\overrightarrow{p_{\perp c\bar{c}}} = \overrightarrow{p_{\perp c}} + \overrightarrow{p_{\perp \bar{c}}}$. For comparison, this is a Dirac delta function in the leading-order approximation to $c\bar{c}$ production. In contrast, double-parton scattering mechanism gives a broad distribution extending to large transverse momenta. NLO corrections obviously destroy the δ-like leading-order correlation. Similar distributions for $D\bar{D}$ seem useful observables to identify the DPS contributions [21].

So far, we have calculated cross section in a simple leading-order approach. A better approximation would be to include multiple gluon emissions. This can be done *e.g.* in soft gluon resummation or in the $k_{\rm t}$-factorization approach. For example, the second approach does not lead to large changes in shape of neither distributions in rapidity nor of distributions in transverse momentum of c ($\bar{c}$) (see *e.g.* [14]) compared to the collinear approach. It is expected, however, to change distributions in transverse momentum of $c\bar{c}$ or in azimuthal angle between c and $\bar{c}$ [14].

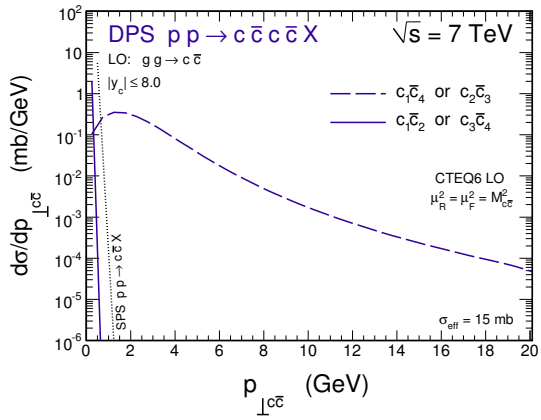

Fig. 17. Distribution in transverse momentum of $c\bar{c}$ pairs from the same parton scattering and from different parton scatterings at $\sqrt{s} = 7$ TeV.

5. Conclusions

We have calculated inclusive spectra of nonphotonic electrons/positrons for RHIC energy in the framework of the $k_{\rm t}$-factorization. We have concentrated on the dominant gluon–gluon fusion mechanism and used unintegrated gluon distribution functions from the literature. Special emphasis was devoted to the Kwieciński unintegrated gluon (parton) distributions. In this formalism, using unintegrated quark and antiquark distributions, one can calculate also the quark–antiquark annihilation process including transverse momenta of initial quarks/antiquarks.

When calculating spectra of charmed (D, D^*) and bottom (B, B^*) mesons, we have used Peterson [9] and Braaten *et al.* [10] fragmentation functions. We have used recent fits to the CLEO [3] and BaBar [4] collaborations data for decay functions of heavy mesons.

Our results have been compared with experimental data measured recently by the PHENIX and STAR collaborations at RHIC. A reasonable description of the data at large transverse momenta of electrons/positrons has been achieved. We have discussed uncertainties related to the choice of the factorization and renormalization scales as well as those related to the fragmentation process. Although the uncertainty bands are rather large, there seems to be a missing strength at lower electron/positron transverse momenta.

We have discussed also correlations of charmed mesons and dielectrons at the energy of recent RHIC experiments. We have calculated the spectra in dielectron invariant mass, in azimuthal angle between electron and positron as well as the distribution in transverse momentum of the pair. The uncertainties due to the choice of UGDFs, choice of the factorization and renormalization scales, have been discussed. We have obtained good description of the dielectron invariant mass distribution measured recently by the PHENIX Collaboration at RHIC.

At RHIC, the contribution of electrons from Drell–Yan processes is only slightly smaller than that from the semileptonic decays. The distributions in azimuthal angle between electron and positron and in the transverse momentum of the dielectron pair from both processes are rather similar. It was found that the distribution in azimuthal angle strongly depends on dielectron invariant mass.

We have also included exclusive central-diffractive contribution discussed recently in the literature. At the rather low RHIC energy it gives, however, a very small contribution to the cross section and can be safely ignored.

The QED double-elastic, double-inelastic, elastic–inelastic and inelastic–elastic processes give individually rather small contribution but when added together are not negligible especially at low dielectron invariant masses, where some strength is missing.

The exclusive production of $c\bar{c}$ pairs is interesting by itself. We have discussed corresponding formalism as well as some results for RHIC and LHC energies. However, experimental identification of the mechanism may be not easy as the final hadronic state is more complicated and will compete with inclusive central diffractive production of $c\bar{c}$.

We have discussed also production of two pairs of $c\bar{c}$. We have found very quickly rising cross section for the two-pair production as a function of center-of-mass energy. The two-pair production must, therefore, give a sizeable contribution to inclusive charm production. This point requires further studies.

We have discussed some promissing observables which seem useful in identifying the DPS production of two pairs of $c\bar{c}$. In Ref. [21], we have considered also corresponding observables for charmed mesons. Another option would be to study production of the same-sign charged leptons. We expect that semileptonic decays are the main source for semi-hard muons or electrons. Furthermore, this contribution can, in principle, be separated experimentally by taking into account that the secondary vertices are shifted with respect to the primary ones. This should allow a separation of the semileptonic "signal" from other possible sources of dilepton continuum.

REFERENCES

[1] J. Adams *et al.* [STAR Collaboration], *Phys. Rev. Lett.* **94**, 062301 (2005); B.I. Abelev *et al.* [STAR Collaboration], *Phys. Rev. Lett.* **98**, 192301 (2007).

[2] A. Adare *et al.* [PHENIX Collaboration], *Phys. Rev. Lett.* **97**, 252002 (2006) [arXiv:hep-ex/0609010].

[3] N.E. Adam *et al.* [CLEO Collaboration], *Phys. Rev. Lett.* **97**, 251801 (2006) [arXiv:hep-ex/0604044].

[4] B. Aubert *et al.* [BaBar Collaboration], *Phys. Rev.* **D69**, 111104(R) (2004).

[5] D. Acosta *et al.* [CDF II Collaboration], *Phys. Rev. Lett.* **91**, 241804 (2003).

[6] A. Adare *et al.* [PHENIX Collaboration], *Phys. Rev. Lett.* **97**, 252002 (2006).

[7] A. Adare *et al.* [PHENIX Collaboration], *Phys. Lett.* **B670**, 313 (2009).

[8] J. Kwieciński, *Acta Phys. Pol. B* **33**, 1809 (2002); A. Gawron, J. Kwieciński, *Acta Phys. Pol. B* **34**, 133 (2003); A. Gawron, J. Kwieciński, W. Broniowski, *Phys. Rev.* **D68**, 054001 (2003).

[9] C. Peterson, D. Schlatter, I. Schmitt, P.M. Zerwas, *Phys. Rev.* **D27**, 105 (1983).

[10] E. Braaten, K. Cheung, S. Fleming, T.C. Yuan, *Phys. Rev.* **D51**, 4819 (1995).

[11] M. Cacciari, P. Nason, R. Vogt, *Phys. Rev. Lett.* **95**, 122001 (2005).

[12] M. Łuszczak, R. Maciuła, A. Szczurek, *Phys. Rev.* **D79**, 034009 (2009).

[13] R. Maciuła, A. Szczurek, G. Ślipek, *Phys. Rev.* **D83**, 054014 (2011).

[14] M. Łuszczak, A. Szczurek, *Phys. Rev.* **D73**, 054028 (2006).

[15] S. Catani, M. Ciafaloni, F. Hautmann, *Nucl. Phys.* **B366**, 135 (1991); J.C. Collins, R.K. Ellis, *Nucl. Phys.* **B360**, 3 (1991); R.D. Ball, R.K. Ellis, *J. High Energy Phys.* **0105**, 053 (2001).

[16] C. Amsler *et al.* [Partilce Data Group], *Phys. Lett.* **B667**, 1 (2008).

[17] X. Lin [STAR Collaboration], *J. Phys. G* **34**, S821 (2007); A.G. Knospe, Proceeding of the CHARM 2007 workshop, Ithaca, August 5–8, 2007; X. Lin, a talk at the international conference Quark Matter 2008, Jaipur, India, February 4–10, 2009.

[18] A. Mischke *et al.* [STAR Collaboration], *J. Phys. G* **35**, 104117 (2008) [arXiv:0804.4601v1 [nucl-ex]].

[19] M. Łuszczak, R. Maciuła, A. Szczurek, *Phys. Rev.* **D84**, 114018 (2011).

[20] R. Maciuła, R. Pasechnik, A. Szczurek, *Phys. Lett.* **B685**, 165 (2010).

[21] M. Łuszczak, R. Maciuła, A. Szczurek, *Phys. Rev.* **D85**, 094034 (2012) [arXiv:1111.3255 [hep-ph]].

[22] M.A. Kimber, A.D. Martin, M.G. Ryskin, *Eur. Phys. J.* **C12**, 655 (2000); *Phys. Rev.* **D63**, 114027-1 (2001).

[23] R. Maciuła, R. Pasechnik, A. Szczurek, *Phys. Rev.* **D83**, 054014 (2011).

[24] R. Maciuła, R. Pasechnik, A. Szczurek, *Phys. Rev.* **D83**, 114034 (2011).

[25] V.A. Khoze, A.D. Martin, M.G. Ryskin, *Phys. Lett.* **B401**, 330 (1997); A.B. Kaidalov, V.A. Khoze, A.D. Martin, M.G. Ryskin, *Eur. Phys. J.* **C33**, 261 (2004).

[26] A. Dechambre, O. Kepka, C. Royon, R. Staszewski, *Phys. Rev.* **D83**, 054013 (2011).

[27] R. Maciuła, R. Pasechnik, A. Szczurek, arXiv:1109.5517v1 [hep-ph].

[28] R.S. Pasechnik, A. Szczurek, O.V. Teryaev, *Phys. Rev.* **D78**, 014007 (2008).

[29] R.S. Pasechnik, A. Szczurek, O.V. Teryaev, *Phys. Lett.* **B680**, 62 (2009); R.S. Pasechnik, A. Szczurek, O.V. Teryaev, *Phys. Rev.* **D81**, 034024 (2010).

[30] A.G. Shuvaev, V.A. Khoze, A.D. Martin, M.G. Ryskin, *Eur. Phys. J.* **C56**, 467 (2008) [arXiv:0806.1447 [hep-ph]].

[31] A.D. Martin, M.G. Ryskin, *Phys. Rev.* **D64**, 094017 (2001).

[32] A.G. Shuvaev, K.J. Golec-Biernat, A.D. Martin, M.G. Ryskin, *Phys. Rev.* **D60**, 014015 (1999).

[33] M. Glück, D. Jimenez-Delgado, E. Reya, *Eur. Phys. J.* **C53**, 355 (2008).